

Engineering the carbon and redox metabolism of *Paenibacillus polymyxa* for efficient isobutanol production

Meliawati Meliawati¹  | Daniel C. Volke² | Pablo I. Nikel²  | Jochen Schmid¹ 

¹Institute of Molecular Microbiology and Biotechnology, University of Münster, Münster, Germany

²The Novo Nordisk Foundation Center for Biosustainability, Technical University of Denmark, Kgs. Lyngby, Denmark

Correspondence

Jochen Schmid, Institute of Molecular Microbiology and Biotechnology, University of Münster, Corrensstraße 3, 48149 Münster, Germany.
Email: jochen.schmid@uni-muenster.de

Funding information

Erasmus+, Grant/Award Number: KA131; Open Access Publication Fund of the Universität Münster; Bundesministerium für Bildung und Forschung, Grant/Award Number: 031B0855A

Abstract

Paenibacillus polymyxa is a non-pathogenic, Gram-positive bacterium endowed with a rich and versatile metabolism. However interesting, this bacterium has been seldom used for bioproduction thus far. In this study, we engineered *P. polymyxa* for isobutanol production, a relevant bulk chemical and next-generation biofuel. A CRISPR-Cas9-based genome editing tool facilitated the chromosomal integration of a synthetic operon to establish isobutanol production. The 2,3-butanediol biosynthesis pathway, leading to the main fermentation product of *P. polymyxa*, was eliminated. A mutant strain harbouring the synthetic isobutanol operon (*kdcA* from *Lactococcus lactis*, and the native *ilvC*, *ilvD* and *adh* genes) produced 1 g L^{-1} isobutanol under microaerobic conditions. Improving NADPH regeneration by overexpression of the malic enzyme subsequently increased the product titre by 50%. Network-wide proteomics provided insights into responses of *P. polymyxa* to isobutanol and revealed a significant metabolic shift caused by alcohol production. Glucose-6-phosphate 1-dehydrogenase, the key enzyme in the pentose phosphate pathway, was identified as a bottleneck that hindered efficient NADPH regeneration through this pathway. Furthermore, we conducted culture optimization towards cultivating *P. polymyxa* in a synthetic minimal medium. We identified biotin (B7), pantothenate (B5) and folate (B9) to be mutual essential vitamins for *P. polymyxa*. Our rational metabolic engineering of *P. polymyxa* for the production of a heterologous chemical sheds light on the metabolism of this bacterium towards further biotechnological exploitation.

INTRODUCTION

The increasing energy demand and concerns over the environmental impacts of fossil-based fuels have given biofuels from renewable resources a rising interest. Bio-based production of renewable alternatives, such as ethanol and isobutanol, has been developed by adopting biotechnological approaches (Gehrman & Tenhumberg, 2020; Su et al., 2020). Compared to ethanol, higher alcohols such as isobutanol have a greater energy density, as well as lower hygroscopicity, volatility and corrosivity, which increases their attractiveness as advanced biofuels. Furthermore, isobutanol is

a versatile solvent necessary for various applications, such as the production of specialty chemicals, surface coatings and adhesives (Fu et al., 2021).

Isobutanol is a four-carbon, branched chain aliphatic alcohol that is not produced naturally in significant quantities, although some microbes such as *Saccharomyces cerevisiae* can produce negligible amounts of this alcohol (Dickinson et al., 1997, 1998). Therefore, a metabolic engineering approach is required to achieve *in vivo* production of isobutanol. This can be realized by introducing the last two steps of the Ehrlich pathway: decarboxylation of branched-chain 2-keto acids to aldehydes by 2-keto acid decarboxylase

(KDC; the *kdcA* or *kivD* gene products), and subsequent reduction of aldehydes to alcohols by alcohol dehydrogenase (ADH; the *adh* gene product). While ADHs are widespread among bacteria, KDCs are scarce and only a few bacteria possessing KDCs have been identified (De La Plaza et al., 2004; Wei et al., 2013; Werther et al., 2008). Among all of these enzymes, KDCs from *Lactococcus lactis* are the best characterized and have been extensively used for the production of higher alcohols (Atsumi et al., 2010; Tai et al., 2016).

Isobutanol formation involves a series of reactions that starts with the condensation of two molecules of pyruvate to acetolactate, catalysed by acetolactate synthase (ALS; the *alsS* gene product; Figure 1). Acetolactate is converted to 2,3-dihydroxyisovalerate by ketol-acid reductoisomerase (KARI; the *ilvC* gene product), which is further dehydrated by dihydroxyacid dehydratase (DHAD; the *ilvD* gene product) to 2-ketoisovalerate, the penultimate precursor for L-valine biosynthesis. Subsequent decarboxylation by KDC forms isobutyraldehyde, which is finally reduced to isobutanol by the action of ADH. Overexpression of *kdcA* from *L. lactis* in combination with the native *alsS*, *ilvC*, *ilvD* and *adh* is a commonly used strategy to achieve heterologous production of isobutanol (Gu et al., 2021). Furthermore, the elimination of competing

pathways and process optimization have been extensively investigated to further increase the product titre. Microbial production of isobutanol has been studied in different microorganisms, such as *Escherichia coli* (Smith & Liao, 2011), *Pseudomonas putida* (Ankenbauer et al., 2021), *Zymomonas mobilis* (Qiu et al., 2020), *Bacillus licheniformis* (Zhan et al., 2021), *Bacillus subtilis* (Li et al., 2012), *Corynebacterium glutamicum* (Zhan et al., 2021), *Geobacillus thermoglucosidasius* (Lin et al., 2014), *Pichia pastoris* (Siripong et al., 2018) and *Saccharomyces cerevisiae* (Park et al., 2014). Notably, high titre isobutanol production ($>20\text{ g L}^{-1}$) has been reported for engineered *E. coli* (Atsumi et al., 2008). Implementation of in situ product removal alleviated the isobutanol toxicity and thus realized a titre of about 50 g L^{-1} by engineered *E. coli* and *C. glutamicum* (Baez et al., 2011; Yamamoto et al., 2013). For many other strains, the reported titres are still relatively low to be considered relevant at an industrial scale.

The soil bacterium *P. polymyxa* is a facultative anaerobe known to naturally produce 2,3-butanediol (2,3-BDO) at high (up to 110 g L^{-1}) titres (Häßler et al., 2012). Despite its versatile metabolism and biochemical capability, research on *P. polymyxa* has been circumscribed to its isolation from natural habitats and characterization of antimicrobial activities

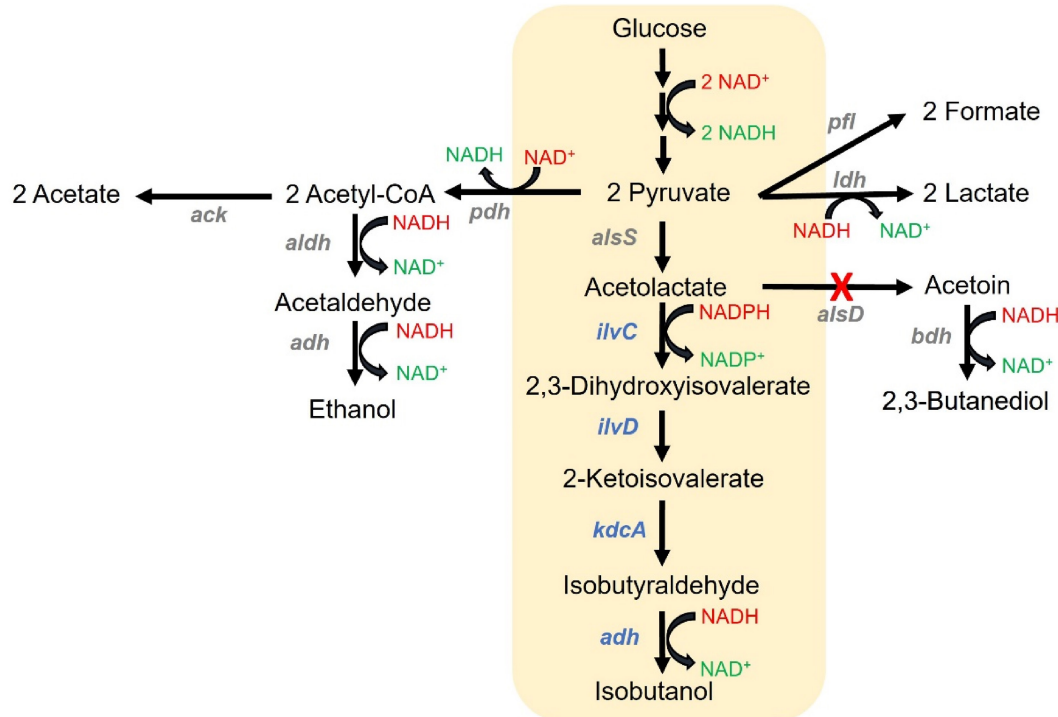


FIGURE 1 Overview of the mixed acid pathway in *Paenibacillus polymyxa* and the engineered isobutanol pathway (highlighted in an orange box). The genes given in blue are overexpressed from a synthetic operon in place of *alsD* to drive isobutanol formation and eliminate the 2,3-BDO pathway. The *ilvC*, *ilvD* and *adh* are native to *P. polymyxa*, while *kdcA* from *Lactococcus lactis* is heterologously expressed. The targeted pathway for isobutanol production is highlighted in grey. *ack*, acetate kinase; *adh*, alcohol dehydrogenase; *aldh*, aldehyde dehydrogenase; *alsD*, acetolactate decarboxylase; *alsS*, acetolactate synthase; *bdh*, butanediol dehydrogenase; *ilvC*, ketol-acid reductoisomerase; *ilvD*, dihydroxyacid dehydratase; *kdcA*, branched-chain alpha-ketoacid decarboxylase; *ldh*, lactate dehydrogenase; *pdh*, pyruvate dehydrogenase; *pfl*, pyruvate-formate lyase.

(Blombach et al., 2021). Only limited knowledge is available in regard to its metabolism, although several studies have investigated its 2,3-BDO and exo-polysaccharide biosynthesis (Okonkwo et al., 2020; Schilling et al., 2022). For a long time, the lack of genetic tools hindered the study of *P. polymyxa* and development for biotechnological applications. We developed a CRISPR-Cas9-based genome editing tool specifically tailored for this bacterium (Rütering et al., 2017). Adopting this toolset in this study, we provide a first-case example of implementing a synthetic pathway for the production of a non-natural compound in *P. polymyxa*. In particular, engineering of *P. polymyxa* for isobutanol production is a promising strategy, as this pathway uses acetolactate as one of the main intermediates, similar to 2,3-BDO biosynthesis, which is the main fermentative pathway of *P. polymyxa* (Figure 1). In contrast to acetolactate conversion to 2,3-dihydroxyisovalerate in the isobutanol pathway, this intermediate is decarboxylated to acetoin and finally reduced to 2,3-BDO in the butanediol biosynthesis. In addition, small amounts of lactate, ethanol, formate and acetate are produced from the mixed acid fermentative pathway (Schilling et al., 2020). Therefore, metabolic engineering strategies to eliminate the formation of 2,3-BDO and other by-products, as well as redirection of the metabolic flux towards isobutanol formation, are essential.

In this study, we demonstrated the rational metabolic engineering of *P. polymyxa* towards isobutanol production. We combined in vitro enzyme assays with proteomic analysis to investigate potential bottlenecks, and these findings were used to further optimize the pathways towards improving product titres. Additionally, we developed a synthetic minimal medium for *P. polymyxa* to reduce production costs. Previous works on *P. polymyxa* relied on the cultivation in rich complex media, which often contain a high amount of yeast extract and peptone, rather expensive components for bulk chemicals production. Here, we provide insights into the complex metabolism of *P. polymyxa* and describe a first-case example of engineering the bacterium for production of a heterologous compound.

EXPERIMENTAL PROCEDURES

Bacterial strains

Paenibacillus polymyxa DSM 365 was obtained from the German Collection of Microorganisms and Cell Culture (DSMZ), Braunschweig, Germany. *E. coli* Turbo™ (New England Biolabs) was used for plasmid cloning and *E. coli* S17-1 (ATCC 47055) was used for the DNA transfer to *P. polymyxa* via conjugation. The strains were cultivated in LB medium (10 g L^{-1} peptone,

5 g L^{-1} yeast extract and 5 g L^{-1} NaCl) unless stated otherwise. The medium was supplemented with $50\text{ }\mu\text{g mL}^{-1}$ of neomycin and $40\text{ }\mu\text{g mL}^{-1}$ of polymyxin when necessary. *P. polymyxa* was routinely cultivated at 30°C and *E. coli* strains at 37°C unless stated otherwise. The strains were stored in 24% (v/v) glycerol at -80°C for long-term storage. All strains used in this study are listed in Table S1.

Strain engineering

All plasmids generated in this study were constructed by the isothermal assembly and transferred to *P. polymyxa* via conjugation, as previously described (Meliawati et al., 2022). The genome modifications were facilitated by the CRISPR-Cas9-based system developed for *P. polymyxa* (Rütering et al., 2017). In brief, the guide RNA (gRNA) for targeted genome editing was designed by using the Benchling CRISPR Design Tool. Approximately, 1 kb up- and downstream homologous flanks were used as the repair template. For genome integration, the genes of interest were placed in between the homologous repair template. For initial screening of the mutants, colony PCR (cPCR) was performed using primers which bind outside of the homologous repair template. Subsequently, the genomic DNA (gDNA) of the mutant strain was isolated and the targeted region was amplified via PCR and the genotype was verified via sequencing.

The *kdcA* gene, which is essential for isobutanol production, was obtained from the gDNA of *L. lactis* (Smit et al., 2005). Other genes such as *ilvC*, *ilvD* and *adh* were amplified from gDNA obtained from *P. polymyxa* DSM 365. The synthetic operon was constructed by combining the native ribosome binding site (RBS) sequences and the open reading frames (ORFs) of *ilvC*, *ilvD* and *adh*, as well as the ORF of *kdcA* in one operon. No additional RBS was added for *kdcA*, as the RBS of the gene that it replaced (*alsD* or *bhd*) was used. All primers and plasmids used in this study are listed in Tables S1 and S2.

Microtiter plate cultivations

Growth analysis for evaluation of the isobutanol toxicity and optimization of cultivation media were performed in 96-well microtiter plates (Greiner-CELLSTAR). To test the isobutanol toxicity, a single colony was used to inoculate a 13 mL tube containing 3 mL of isobutanol fermentation medium. The culture was grown overnight at 37°C and 250 rpm. Subsequently, $2\text{ }\mu\text{L}$ of the overnight culture was inoculated into 200 μL fermentation medium supplemented with different concentrations of isobutanol,

ranging from 0 to 20 g L⁻¹. The plate was sealed with a Breathe-Easy sealing membrane (Sigma-Aldrich). The cultures were cultivated at 37°C with medium continuous shaking for 48 h (ELX808; BioTek), and the OD₆₀₀ was recorded every 15 min. Growth profiles and kinetic parameters were analysed using the QuruE software (Wirth et al., 2023).

For the media optimization, the precultures were prepared in their respective media. The isobutanol fermentation medium was utilized as the rich medium; de Bont medium was used as the base for the minimal medium (Hartmans et al., 1989). de Bont medium consisted, per litre, the following components: 1.55 g K₂HPO₄, 0.85 g NaH₂PO₄·2H₂O, 2.0 g (NH₄)₂SO₄, 0.1 g MgCl₂·6H₂O, 10 mg EDTA, 2 mg ZnSO₄·7H₂O, 1 mg CaCl₂·2H₂O, 5 mg FeSO₄·7H₂O, 0.2 mg Na₂MoO₄·2H₂O, 0.2 mg CuSO₄·5H₂O, 0.4 mg CoCl₂·6H₂O and 1 mg MnCl₂·2H₂O. The medium was supplemented with 20 g L⁻¹ glucose, with the addition of either 0.05 g L⁻¹ yeast extract, 0.05 g L⁻¹ peptone, 0.1 g L⁻¹ amino acid mix (Teknova) or 1:10,000 Wolfe's vitamin solution, as indicated. Furthermore, for the evaluation of single component of the vitamin mix, the minimal medium was instead supplemented with vitamin B1 (5 µg L⁻¹), B2 (5 µg L⁻¹), B3 (5 µg L⁻¹), B5 (5 µg L⁻¹), B6 (10 µg L⁻¹), B7 (2 µg L⁻¹), B9 (2 µg L⁻¹) or B12 (0.1 µg L⁻¹).

Isobutanol production and analysis

The fermentation medium composition was adapted from previous studies (Okonkwo et al., 2017; Schilling et al., 2020). The medium consisted of 60 g L⁻¹ glucose, 5 g L⁻¹ yeast extract, 5 g L⁻¹ peptone, 0.2 g L⁻¹ MgSO₄·7H₂O, 3.5 g L⁻¹ KH₂PO₄ and 2.5 g L⁻¹ K₂HPO₄. All medium components were obtained from Carl Roth GmbH (Germany) unless indicated differently. *P. polymyxa* strains were streaked on LB agar plates and incubated overnight at 30°C. A single colony was used to inoculate a 13-mL tube containing 3 mL fermentation medium, and cultivated overnight at 37°C and 250 rpm. Subsequently, 30 µL of this preculture was transferred into a fresh 3 mL fermentation medium in a 10-mL glass tube and cultivated at 37°C, 250 rpm for 48 h. For shake flask cultivation, 50 µL preculture was used to inoculate 50 mL medium in a 250 mL shake flask. Following the fermentation, 1 mL of the culture was centrifuged at 19,000 g for 5 min and the supernatant was filtered through a 0.2-µm PTFE filter. The concentration of glucose and fermentative products were measured with HPLC-UV-RID (Dionex, USA) equipped with a Rezex ROA-H⁺ organic acid column (300 mm × 7.8 mm, Phenomenex, USA). The column temperature was set to 70°C, and 2.5 mM H₂SO₄ was used as the mobile phase with a flow rate of 0.5 mL min⁻¹ and 55 min run time.

In vitro analysis

The strains were cultivated in the isobutanol fermentation medium as described above. The cells were harvested at different time points which represented different growth phases: exponential (6 h), late exponential (10 h) and stationary phase (24 h). First, the cells were centrifuged at 4000 g at 4°C for 10 min. Subsequently, the cells were washed with PBS buffer, centrifuged again under the same condition and then the pellet was resuspended in 0.5 mL PBS buffer. Disruption of cells was performed with a bead beater at 6000 rpm for 20 s (PRECELLYS 24, Bertin Technologies), followed by centrifugation at 17,000 g at 4°C for 2 min. Protein concentration in the supernatant was determined using the Bradford assay (Bradford, 1976), and the supernatant was used for further experiments with the cell extract. For the investigation of the upper isobutanol pathway, 5 µg protein was added into a reaction mixture containing 30 mM pyruvate, 0.5 mM NAD(P)H, 5 mM MgSO₄, 0.2 mM thiamine pyrophosphate (TPP) and PBS buffer, with a total reaction volume of 200 µL. For the lower isobutanol pathway, 30 mM 2-ketoisovalerate was used instead of pyruvate. The assay was performed in a microtiter plate and the absorption at 340 nm at 37°C was recorded every 30 s (ELX808; BioTek).

Proteomics

Paenibacillus polymyxa strains were cultivated in the fermentation medium as described above, and harvested at desired time points. Two millilitres of culture was centrifuged at 17,000 g for 5 min and the pellet was stored at -20°C until further use. For the cell lysis, two pieces of 3-mm zirconium oxide beads and 100 µL of lysis buffer (6.0 M guanidinium hydrochloride, 5 mM tris(2-carboxyethyl)phosphine, 10 mM CICH₂CONH₂ and 100 mM Tris-HCl pH 8.0) were added to the cell pellet and the cells were lysed with TissueLyser (Qiagen) at 25 Hz for 5 min. The mixture was incubated in a heating block at 99°C and 2000 rpm for 10 min and then centrifuged at 15,000 g for 10 min. Subsequently, 50 µL of supernatant was added with 50 µL of 50 mM NH₄HCO₃. Protein concentration was measured using micro BCA Protein Assay Kit (Thermo Scientific) following the standard protocol. Protein digestion was done with 20 µL of 0.1 µg µL⁻¹ Trypsin/Lys-C protease mix (Promega) at 37°C for 12 h. The reaction was stopped by adding 10 µL of 10% (v/v) trifluoroacetic acid (TFA) followed by centrifugation at 15,000 g for 15 min. The peptides were then purified by StageTips purification steps (Rappaport et al., 2007). The C18 filter was placed onto a 200 µL C18 StageTips and then sequentially washed with 20 µL MeOH, 20 µL buffer B (80% (v/v) acetonitrile, 0.1% (v/v) formic acid) and 20 µL buffer A (3% (v/v) acetonitrile, 1% (v/v) TFA) by centrifugation at 1000 g for 1 min. The peptides were

loaded through the C18 column at 1500 g for 2 min and washed two times with 20 µL of buffer A at 1500 g for 1 min. The elution was done with 2 × 20 µL of buffer B at 1000 g for 1 min. The samples were concentrated until a volume of ~5 µL in an Eppendorf concentrator, then 0.1% (v/v) formic acid was added until a final volume of 20 µL.

Subsequently, the peptides were loaded onto a 2 cm C18 trap column (ThermoFisher 164946), connected in-line to a 15 cm C18 reverse-phase analytical column (Thermo EasySpray ES904) using 0.1% (v/v) formic acid at 750 bar, in a Thermo EasyLC 1200 HPLC system with a column oven operating at 30°C. The peptides were eluted over a 70-min gradient ranging from 10% to 60% (v/v) of Buffer B at 250 nL min⁻¹, and the Orbitrap Exploris instrument (Thermo Fisher Scientific) was run in DIA mode with FAIMS ProTM Interface (ThermoFisher Scientific) with CV of -45V. Full MS spectra were collected at a resolution of 120,000, with an AGC target of 300% or maximum injection time set to 'auto' and a scan range of 400–1000 m/z. The MS2 spectra were obtained in DIA mode in the orbitrap operating at a resolution of 60,000, with an AGC target of 1000% or maximum injection time set to 'auto', a normalized HCD collision energy of 32. The isolation window was set to 6 m/z with a 1 m/z overlap and window placement on. Each DIA experiment covered a range of 200 m/z resulting in three DIA experiments (400–600, 600–800 and 800–1000 m/z). Between the DIA experiments, a full MS scan was performed. MS performance was verified for consistency by running complex cell lysate quality control standards, and chromatography was monitored to check for reproducibility. The raw files were analysed using SpectronautTM (version 16.2) spectra were matched against the Ppiso-5 protein database. Dynamic modifications were set as Oxidation (M) and Acetyl on protein N-termini. Cysteine carbamidomethyl was set as a static modification. All results were filtered to a 1% FDR, and protein quantitation was done on the MS1 level. The data was normalized by RT dependent local regression model (Callister et al., 2006) and protein groups were inferred by IDPicker. Statistical analysis of the proteomics data was performed with the two-tailed student's *t*-test for unequal variances and only the data with a *p*<0.05 was considered for further data interpretation. The mass spectrometry proteomics data have been deposited to the ProteomeXchange Consortium via the PRIDE (Perez-Riverol et al., 2022) partner repository with the dataset identifier PXD048679.

RESULTS AND DISCUSSION

Integration of a synthetic operon to establish isobutanol production

By employing the pCasPP system, we integrated *kdcA* from *L. lactis* into the locus of *alsD* in the chromosome of *P. polymyxa* (Rütering et al., 2017). Thereby, the open

reading frame of *alsD*, which encodes the acetolactate decarboxylase, was directly replaced by the one of *kdcA*, thus eliminating the 2,3-BDO production, which is the main fermentative product of *P. polymyxa*. In addition, the integration circumvents the use of plasmids-based expression and alleviates the need for selection pressure for plasmid maintenance. Here, *kdcA* is placed under the transcriptional control of the native promoter of *alsD*, which is induced in the late exponential phase and under anaerobic conditions. Hence, this construct allows for a period of cell growth before entering the isobutanol production phase, thus decoupling growth and production. Under micro-aerobic conditions, the *kdcA*-harbouring strain (Ppiso-1) produced 0.15 g L⁻¹ of isobutanol.

Paenibacillus polymyxa has four copies of putative lactate dehydrogenases (*ldh*) that might contribute to lactate production. As deletion of one of the *ldh* was shown to improve growth and 2,3-BDO production (Schilling et al., 2020), we deleted this particular gene and generated the Ppiso-2 strain. Deletion of the *ldh* reduced the lactate formation and increased the titre to 0.19 g L⁻¹. Subsequent insertion of an additional copy of *kdcA* in the locus of *bdh* (Ppiso-3) only resulted in a negligible increase of isobutanol titres, which suggests that precursors supply might in fact be the limiting factor. Next, we integrated a synthetic operon consisting of *kdcA* of *L. lactis*, as well as *ilvC*, *ilvD* and *adh* from *P. polymyxa*. Thus, two copies of the native genes (*ilvC*, *ilvD* and *adh*) were present in the *P. polymyxa* genome. Two different ADHs were investigated since previous studies have reported different affinity of ADHs towards isobutyraldehyde, which subsequently influences its conversion rate to isobutanol. Besides *yugJ*, encoding an iron-containing alcohol dehydrogenase, whose orthologue in *Bacillus licheniformis* was reported to have the highest substrate affinity (Zhan et al., 2021), we chose *adhA*, an orthologue of the ADH commonly used for isobutanol production in engineered *E. coli* (Smith & Liao, 2011). Cultivation of the strains carrying the operon with *yugJ* (Ppiso-4) or *adhA* (Ppiso-5) resulted in 0.68 and 1.1 g L⁻¹ isobutanol production respectively (Figure 2A).

Besides isobutanol, the engineered strains also produced other byproducts such as ethanol, lactate, acetate and interestingly meso-BDO. *P. polymyxa* is known for its ability to produce stereoisomer-pure R,R-BDO, but not meso-BDO, as its genome does not encode an acetooin racemase or diacetyl reductase, which are thought to be essential for its production (Petrov & Petrova, 2021). As meso-BDO is produced under micro-aerobic conditions in the absence of the R,R-BDO pathway, this hints at its importance for NAD⁺ regeneration. Consequently, shake flask cultivation of the Ppiso-5 strain, which imposes less oxygen limitation than the tube cultivation, resulted in an 11-fold decrease of meso-BDO while maintaining the isobutanol titre (Figure 2A). Although ethanol production is theoretically a more efficient way for NAD⁺

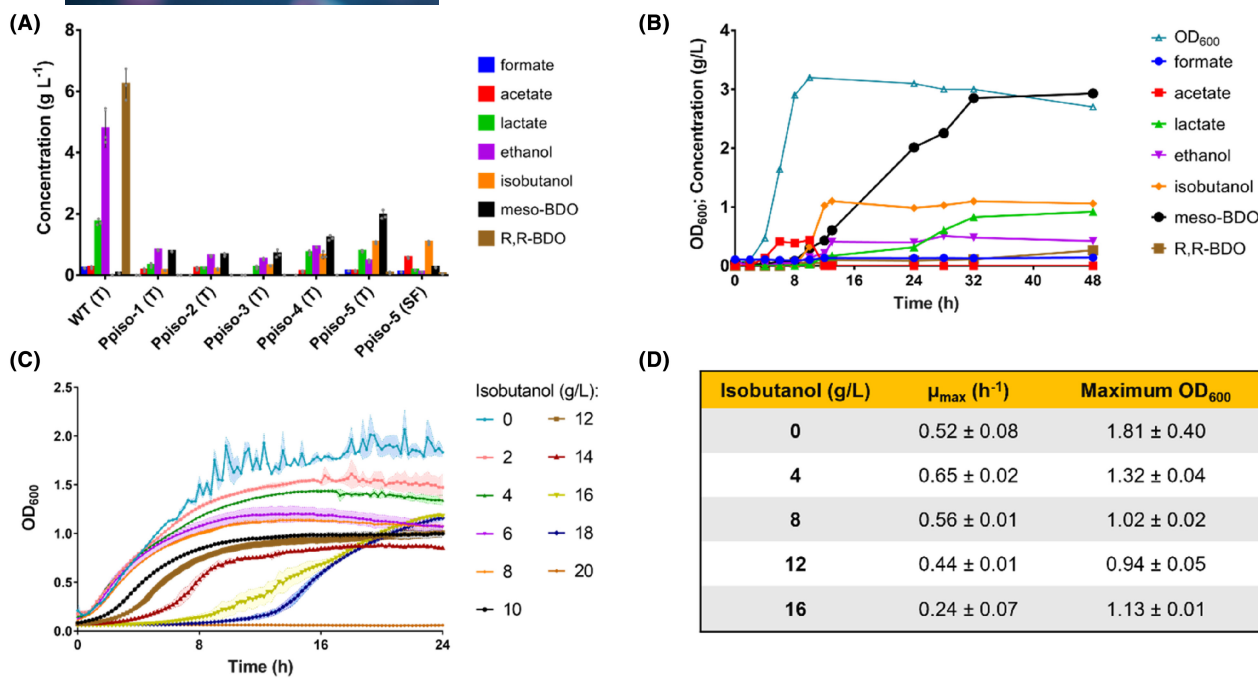


FIGURE 2 (A) Product profiles of wild type (WT) and engineered isobutanol-producing *Paenibacillus polymyxa* (Ppiso) strains after 48-h cultivations in test tubes (T) or shake flasks (SF). (B) Biomass density (OD_{600}) and product profiles of Ppiso-5 strain during cultivation. (C, D) Growth profile of *P. polymyxa* supplemented with varying concentrations of isobutanol. Detailed information on the growth profile in a medium supplemented with isobutanol is available in Table S4. The bar and line graphs indicate mean values, and the error bars indicate the standard deviation obtained from three biological replicates.

regeneration, *P. polymyxa* seems to favour BDO production (Figure S1), as observed in a previous study (Schilling et al., 2020). This behaviour might indicate the high activity of ALS. Many *Bacilli*, such as *B. subtilis* and *B. licheniformis*, are known to have highly active ALS enzymes (Atsumi et al., 2009; Huo et al., 2018). Hence, it is plausible that the meso-BDO originated from the spontaneous reaction of acetolactate into diacetil, which was then converted to acetoin and further to meso-BDO (Dorau et al., 2019).

Evaluation of potential metabolic bottlenecks and competing pathways

The production profile of the fermentative compounds revealed that isobutanol synthesis occurred in a very narrow window from 8 to 12 h (Figure 2B). About 0.33 g L⁻¹ isobutanol was detected after 10 h of cultivation and the amount tripled at 12 h. However, the production stalled afterwards and no significant increase in isobutanol titre was observed. In contrast, other fermentation products, such as, meso-BDO and lactate, continued to increase until around 32 h of cultivation. By the end of the cultivation, a high amount of glucose was still present and thus the stop in isobutanol production was not caused by carbon source limitation (Table S3).

Previous studies have reported isobutanol toxicity and microbial strains showed varying tolerance to isobutanol (Gupta et al., 2020; Wilbanks & Trinh, 2017).

To evaluate whether the stop of isobutanol production was due to toxicity, we cultivated the wild-type strain with different concentrations of isobutanol, ranging from 0 to 20 g L⁻¹ (Figure 2C). The strain was passed directly into the isobutanol-supplemented medium without prior exposure to isobutanol. Higher concentrations than 8 g L⁻¹ isobutanol led to an extended lag phase, most likely because the strain needs time to adapt to the isobutanol-containing media by altering the expression of several genes. However, this was not the case for concentrations below 8 g L⁻¹ and the maximum growth rates (μ_{\max}) remained stable at 0.6–0.8 h⁻¹ (Figure 2D, Table S4). Altogether, this result shows that the toxicity was not responsible for the abrupt interruption of isobutanol production, since the Ppiso-5 strain reached only a concentration of ~1 g L⁻¹ isobutanol.

As toxicity was ruled out to cause the limited isobutanol production, we turned our attention to gene expression and enzyme activity as the limiting factors. To obtain insight about which enzymes are produced and are active at different growth phases, we determined the specific activity of the enzymes of the isobutanol pathway at different growth phases. To this end, we prepared cell lysates from *P. polymyxa* at different time points during cultivation. Furthermore, we divided the pathway into an upper and a lower part for analysis (Figure 3A). As KARI and ADH are NADPH and NADH-dependent, respectively, the enzyme activity of each part was quantified by following the consumption of these cofactors. For the upper part, pyruvate

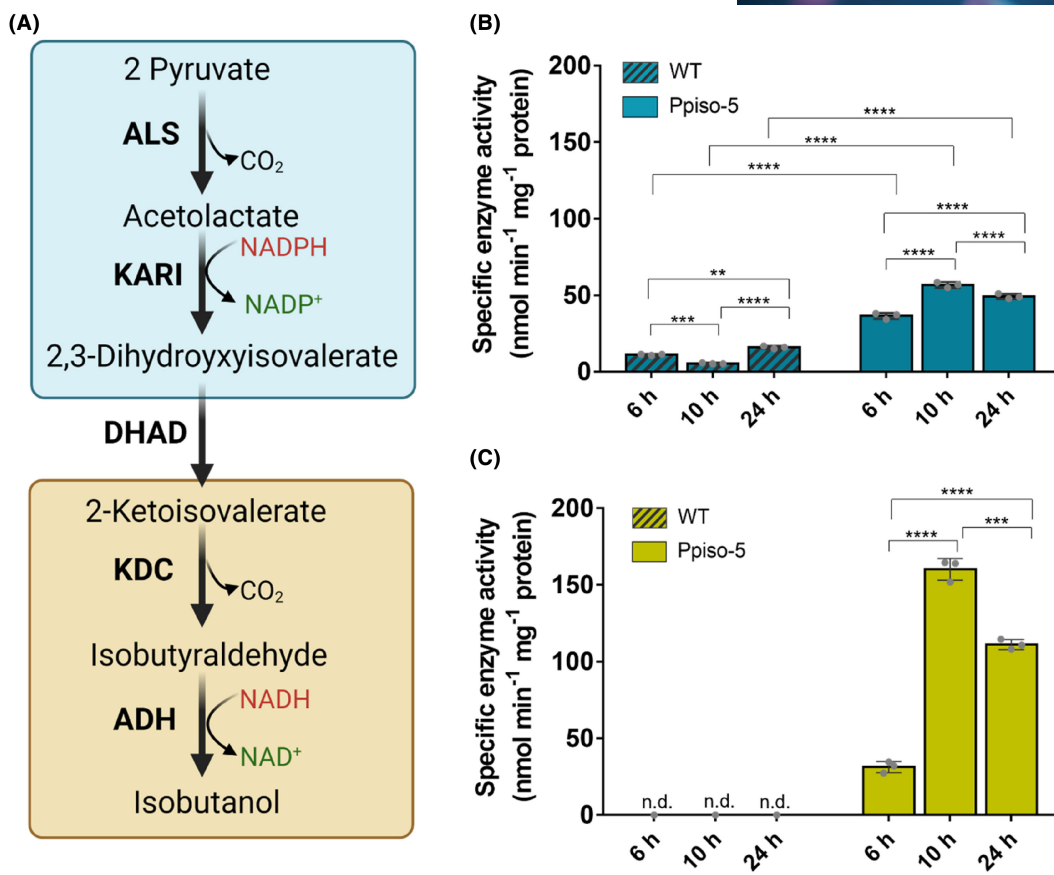


FIGURE 3 Assaying the isobutanol pathway enzymes in *Paenibacillus polymyxa* cell lysate. (A) For the analysis, the pathway was divided into two parts: an upper, NADPH-dependent part (in blue) and a lower NADH-dependent part (in yellow). The combined activity of the enzymes of the upper part was measured with the substrates pyruvate and NADPH (B), while the lower part was probed with 2-ketoisovalerate and NADH (C). The cell lysates were obtained from the Ppiso-5 strain harvested at early exponential (6 h), late exponential (10 h) and stationary growth phases (24 h); n.d., not detected. The bar graphs represent mean values, and the error bars indicate the standard deviation obtained from three biological replicates. A $p < 0.05$ was considered in determining the significant differences between the samples (** $p < 0.01$, *** $p < 0.001$ and **** $p < 0.0001$).

and NADPH were added to the reaction, while for the lower part 2-ketoisovalerate and NADH were supplemented. The activity of all enzymes was measured under substrate saturation conditions. Interestingly, the activity of ALS and KARI, in the upper pathway, was already detected at 6 h with a specific activity of $37 \pm 2 \text{ nmol min}^{-1} \text{ mg}^{-1}$, and the rate increased to 57 ± 2 and $49 \pm 1 \text{ nmol min}^{-1} \text{ mg}^{-1}$ at 10 and 24 h respectively (Figure 3B; Figure S2). The activity of enzymes of the lower pathway part, KDC and ADH, was relatively low at 6 h ($31 \pm 3 \text{ nmol min}^{-1} \text{ mg}^{-1}$) but reached 160 ± 6 and $111 \pm 3 \text{ nmol min}^{-1} \text{ mg}^{-1}$ at 10 and 24 h respectively (Figure 3C, Figure S3). Thus, this observation helps explaining why isobutanol concentration strongly increases around 10 h. These findings suggested that optimization of the expression pattern of the last two steps of the pathway, starting from 2-ketoisovalerate, might enable early isobutanol production, and thus extending the production phase.

Given that the specific activity of the lower pathway is greater than $160 \pm 6 \text{ nmol min}^{-1} \text{ mg}^{-1}$ at the early stationary phase, a productivity of $4.71 \text{ g L}^{-1} \text{ h}^{-1}$

could theoretically be realized at the final biomass concentration ($\text{OD}_{600} = 3$), if precursor supply was not limited. In contrast, the measured productivity was only $0.35 \text{ g L}^{-1} \text{ h}^{-1}$ (Figure S4). As the theoretical productivity far exceeds the measured productivity, we suspected that inadequate precursors supply, that is, pyruvate, NADH or NADPH was limiting the formation of isobutanol.

Engineering redox balance to boost isobutanol biosynthesis

The growth and production profile over time showed an interesting correlation between growth and isobutanol production. It was observed that the cells actively produced isobutanol only during the late exponential growth phase and early stationary phase. While the onset of production is limited by the expression of the genes in the lower part of the isobutanol pathway, as seen before, the abrupt stop of production when entering the stationary phase, while other NADH and

pyruvate-dependent fermentation products are still formed, hints at a limited NADPH supply. This could be caused by reduced flux during the late stationary phase through the tricarboxylic acid (TCA) cycle, which is one of the main generators of cellular NADPH (Spaans et al., 2015). NADPH limitation has been known as a general challenge for isobutanol production, as glycolysis yields two molecules of NADH while isobutanol formation from pyruvate requires one NADPH and one NADH molecule. Previous studies have reported different approaches to overcome this bottleneck, such as overexpression of transhydrogenase, malic enzyme or NAD kinase (Blombach & Eikmanns, 2011; Shi et al., 2013). However, these approaches have met with varying degrees of success, depending on the microbial strain. Therefore, we manipulated the redox balance of *P. polymyxa* for isobutanol production through different approaches.

The conversion of acetolactate to 2,3-dihydroxyisovalerate via the NADPH-dependent KARI is the main reason for the redox imbalance of the isobutanol pathway. Therefore, changing the co-factor specificity of KARI from NADPH to NADH might alleviate this problem. A previous study demonstrated the successful protein engineering of KARI from *E. coli* into an NADH-dependent variant which resulted in improved isobutanol production (Bastian et al., 2011). Similarly, the cofactor specificity of KARI from *L. lactis* was changed (Brinkmann-Chen et al., 2013). As the orthologous form from *L. lactis* is closely related to the one from *P. polymyxa*, both contain a six-residue β 2 α B loop which determines cofactor specificity, the mutations from *L. lactis* were mimicked (Figure S5). To this end, the amino acid sequences were aligned and the R49P, K52L and S53D mutations were applied to the KARI of *P. polymyxa*. These changes in KARI yielded the strain Ppiso-6. Unfortunately, the engineered KARI was detrimental to isobutanol production and reduced the titre (0.32 g L^{-1}) by 70% compared to the Ppiso-5 strain (Table S3). This shows that the beneficial mutations are not readily transferable from one orthologous form to another. By that, random mutagenesis might be necessary to increase the catalytic activity of cofactor-swapped variants to a level close to the wild type (Brinkmann-Chen et al., 2013).

As the approach to switch the redox cofactor dependency of the isobutanol pathway was not successful, we explored other approaches to boost the NADPH generation to ensure sufficient cofactor supply for isobutanol production (Figure 4A). Consequently, we deleted the glucose-6-phosphate isomerase (*pgi*), which is a glycolytic gene responsible for the conversion of glucose-6-phosphate to fructose-6-phosphate in the Embden–Meyerhof–Parnas (EMP) pathway. As *P. polymyxa* does not encode an active Entner–Doudoroff (ED) pathway, the carbon flux is redirected through the pentose phosphate (PP) pathway. The PP

pathway utilizes NADP, whereas the EMP pathway uses NAD. However, the *pgi* deletion in the Ppiso-7 strain did not improve the isobutanol titre compared to the Ppiso-5. Although the by-products were significantly reduced as the titre of meso-BDO, lactate and ethanol decreased by more than 85%. As most *Bacilli* mainly utilize the EMP pathway for glucose metabolism (Wushensky et al., 2018), Ppiso-7 consumed less glucose than the other strains (Table S3). However, the strain seems to have reached fine-tuned activity of the isobutanol pathway, rendering this alcohol as the main fermentation product. Likewise, by-product formation is minimized at the expense of overall lower productivity.

Aiming to pursue higher product titers, we further explored another approach to improve NADPH regeneration by incorporating an NADP-dependent malic enzyme (*maeB*) in the synthetic operon. The malic enzyme is responsible for the decarboxylation of malate to pyruvate and CO_2 , which concomitantly produces NADPH. In addition to improved NADPH regeneration, overexpression of the malic enzyme might also increase the supply of pyruvate, which subsequently could be utilized for the isobutanol formation. This strategy resulted in a 43% increase of isobutanol compared to the Ppiso-5 strain, reaching a final titre of 1.5 g L^{-1} (Figure 4B). Interestingly, the newly designed strain (Ppiso-8) also produced less by-products, in particular, meso-BDO, lactate and ethanol (Table S3).

Proteomics analysis for evaluation of synthetic isobutanol operon

As isobutanol production is not solely dependent on the rationally introduced enzymes, but also relies on glycolysis for precursor supply and different native alcohol dehydrogenases might be involved in the reduction of isobutyraldehyde to isobutanol, we set out to investigate the protein expression pattern in *P. polymyxa* at different growth stages. Proteome analysis of the Ppiso-5 in comparison to the parental strain Δldh showed that besides KARI, the NADPH-consuming proteins were downregulated, allowing KARI to pull the available cellular NADPH towards the isobutanol pathway. However, the strong upregulation of KARI was not accompanied by the upregulation of NADPH-generating enzymes, which might result in NADPH exhaustion in the cells. The two major NADPH-regenerating enzymes, isocitrate dehydrogenase and glucose-6-phosphate 1-dehydrogenase (G6PD), were only upregulated about to 10% (Table S5).

Looking at the enzymes of the isobutanol pathway, expression of KDC, KARI and ADH are induced after 10 h, which explains the effective isobutanol production starting around this time point (Figure 5A). The significant increase of KDC and KARI corresponds to the activation of the *a/sD* promoter, which

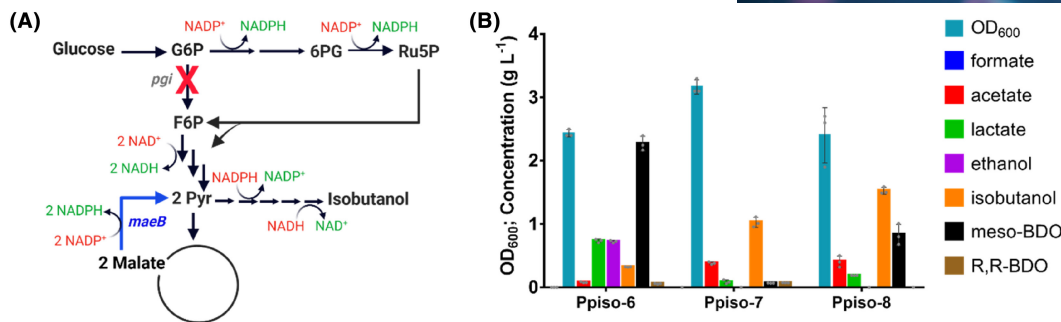


FIGURE 4 Strategies for improved NADPH regeneration to increase isobutanol production. (A) Overview of the central carbon metabolism and synthetic isobutanol pathway in *Paenibacillus polymyxa*. Deletion of glucose-6-phosphate isomerase (*pgi*) would redirect the carbon flux into the pentose phosphate pathway, which generates NADPH. Overexpression of the NADP⁺-dependent malic enzyme (*maeB*) also provides NADPH through the decarboxylation of malate to pyruvate. (B) Product profile of engineered strains upon the implemented NADPH regeneration strategies. The product profile was measured after 48-h cultivation. The bar graphs indicate mean values, and the error bars indicate the standard deviation obtained from three biological replicates.

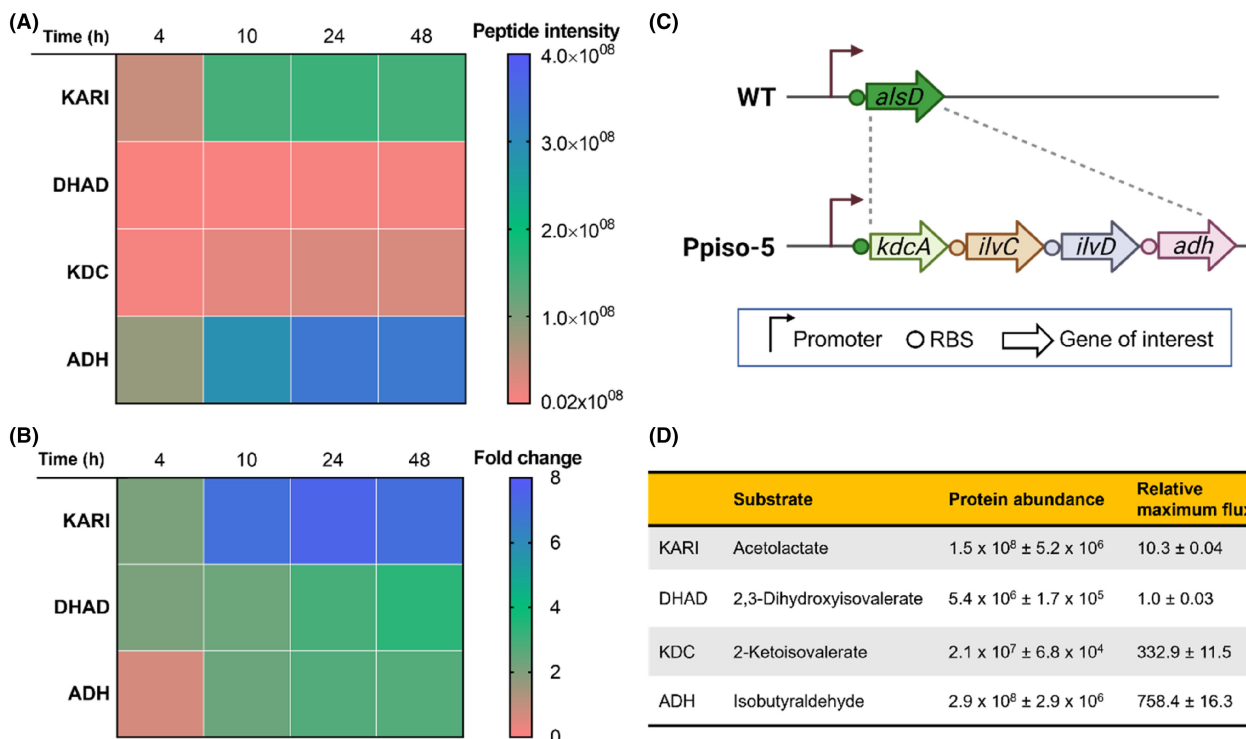


FIGURE 5 (A) Protein abundance of the last four enzymes in the isobutanol pathway and (B) upregulation of KARI, DHAD and ADH compared to the non-producing Δldh strain. (C) The corresponding genes were expressed from a synthetic operon, consisting of *kdcA-ilvC-ilvD-adh*, which was chromosomally integrated into the *Paenibacillus polymyxa* genome replacing the *alsD* and expressed under the control of *alsD* native promoter. (D) The relative maximum flux that can be sustained by the enzymes in the isobutanol pathway. The theoretical maximum flux is estimated by multiplying k_{cat} values from literature with the relative abundance of each enzyme to the total protein in the extract (Bayaraa et al., 2022; Brinkmann-Chen et al., 2013; Gocke et al., 2007; Liu et al., 2013). The flux values were then normalized to the lowest relative maximum theoretical flux (DHAD).

is activated in the post-exponential growth phase (Renna et al., 1993). While KARI has an eightfold higher abundance compared to the Δldh , DHAD and ADH expression is only upregulated around three-fold respectively (Figure 5B; Table S6). This is plausible since in the operon the genes were placed in the order of KDC-KARI-DHAD-ADH (Figure 5C). Consequently, the expression levels of genes encoding DHAD and ADH might be lower due to their distal

position (Lim et al., 2011). While the level of ADH increased over the course of cultivation, the amount of DHAD remained relatively constant. Hence, the maximum flux that can be sustained by the DHAD activity is 10 times less than the preceding reaction catalysed by KARI, suggesting that DHAD might be a potential bottleneck of the pathway (Figure 5D; Table S7). In contrast to ADH, which is part of the fermentative pathways, DHAD is part of the branched-chain amino

acids biosynthesis pathways. This might explain the induction of *adh* in the early stationary phase and the constitutive expression of *dhad*.

Effects of the presence and production of isobutanol on the proteome of *P. polymyxa*

To transform *P. polymyxa* into a bacterial cell factory for the production of isobutanol, it is imperative that the product of the process is well tolerated by the strain. However, in the presence of already low concentration ($<10\text{ g L}^{-1}$), isobutanol results in extended lag phases and lower final biomass concentrations (Figure 2D). Therefore, we set out to analyse the proteomic response of *P. polymyxa* to isobutanol in order to identify the toxicity mechanism and possible engineering strategies to increase the resistance. This study covered about 48% of the theoretical proteome (2674 proteins), including the heterologous KDC. In addition to the wild type, the Δldh strain was also evaluated as this deletion was incorporated into most of the isobutanol-producing strains generated in this study. Only proteins with significant differences ($p < 0.05$) between the sample and control groups were considered for data interpretation and analysis.

The supplementation of isobutanol at low concentrations (2 g L^{-1}) resulted in only a few genes that were differentially expressed by more than fivefold change (Figure 6A,B; Tables S8 and S9). In the wild type, the flagella biosynthesis protein (FliP) was among the most upregulated genes. Increased flagella formation is associated with increased motility and in turn chemotaxis, which is a general toxicity response of bacteria (Colin et al., 2021). A dramatic increase was observed for the mannose-specific PTS system component with nearly 15-fold increase. A recent study identified *manY*, encoding a mannose-specific importer, among the most commonly mutated genes in *E. coli* grown in the presence of *n*-butanol, suggesting a role in general stress tolerance (Lennen et al., 2023). Meanwhile, the formate efflux transporter (*focA*) was upregulated to 17-fold in the Δldh strain in the presence of isobutanol. The efflux pump is known to play an important role in bacterial tolerance, as it facilitates the removal of toxic substances from the cytoplasm (Basler et al., 2018). Although *E. coli* FocA was reported to have a strong preference for formate (Beyer et al., 2013), no information is available for FocA from *P. polymyxa*. Therefore, further investigations are necessary to verify whether it could act on short-chain alcohols such as isobutanol.

The implementation of the synthetic operon and isobutanol production resulted in a strong metabolic impact, as shown by the proteome comparison of Ppiso-5 and the parental strain Δldh after 48 h of cultivation. In total, 402 proteins were found to be downregulated and 280 proteins were upregulated in Ppiso-5 compared

to the Δldh (Figure 6C; Table S10). The enzymes related to ethanol and formate fermentation, such as alcohol dehydrogenases and pyruvate-formate lyase were less expressed, which explains the reduced by-product formation of the isobutanol-producing strain. Besides KDC and KARI, proteins related to biofilm formation and extracellular matrix substances were strongly upregulated. In particular, the Veg protein and GDP-L-fucose synthetase were 11-fold upregulated, as well as the UDP-glucose 6-dehydrogenase which was fivefold more abundant. Biofilm serves multiple functions in the microbial community, including protection against environmental and chemical stressors (Balcazar et al., 2015). Hence, the stimulation of biofilm formation could be a cellular response to cope with the isobutanol presence. Just recently, a fucose-rich exopolysaccharide was reported for *P. polymyxa*, which underpins increased polysaccharide production (Schilling et al., 2022). Furthermore, increased biofilm formation in the presence of alcohol was previously reported for *Bacillus cereus* (Yan et al., 2017).

The proteome analysis of the Ppiso-5 strain showed that the metabolism shifted over the different growth phases (Figure 6D; Table S11). In the early exponential phase, proteins affiliated with the glycolysis, TCA cycle and PP pathway accounted for 3%, 1% and 0.6% of the total proteins respectively. In addition, proteins involved in the production of fermentative metabolites such as acetate, formate, lactate, ethanol, 2,3-BDO and isobutanol, represented 2.5% of the total protein content. During this phase, the cells underwent rapid growth and efficient aerobic respiration, as observed from the highly upregulated TCA cycle compared to the other growth phases. Many enzymes in the TCA cycle were downregulated at the end of the exponential phase, which indicates a slower cycle rate, as the cells shifted from aerobic to microaerobic condition and thus to production of fermentation products. Interestingly, despite the general decrease of the enzymes in the TCA cycle, isocitrate dehydrogenase (IDH) and succinate dehydrogenase (SDH) were upregulated in the later growth phases. These two enzymes catalyse redox reactions and generate NADPH and FADH₂ respectively. Accordingly, the quantity of the ribosomal proteins decreased when growth slowed down while the level of the glycolytic and fermentative enzymes increased (Figure S6).

Furthermore, despite the general increase of the PP pathway by two times at the stationary phase compared to exponential phase, the amount of G6PD remained constant throughout the cultivation. G6PD catalyses the first reaction of the PP pathway by the oxidation of glucose-6-phosphate to 6-phosphogluconolactone, which generates NADPH. This reaction has been reported to be the rate-limiting step that directly controls the PP pathway flux (Stincone et al., 2015). Moreover, the profile of proteins related to the central carbon

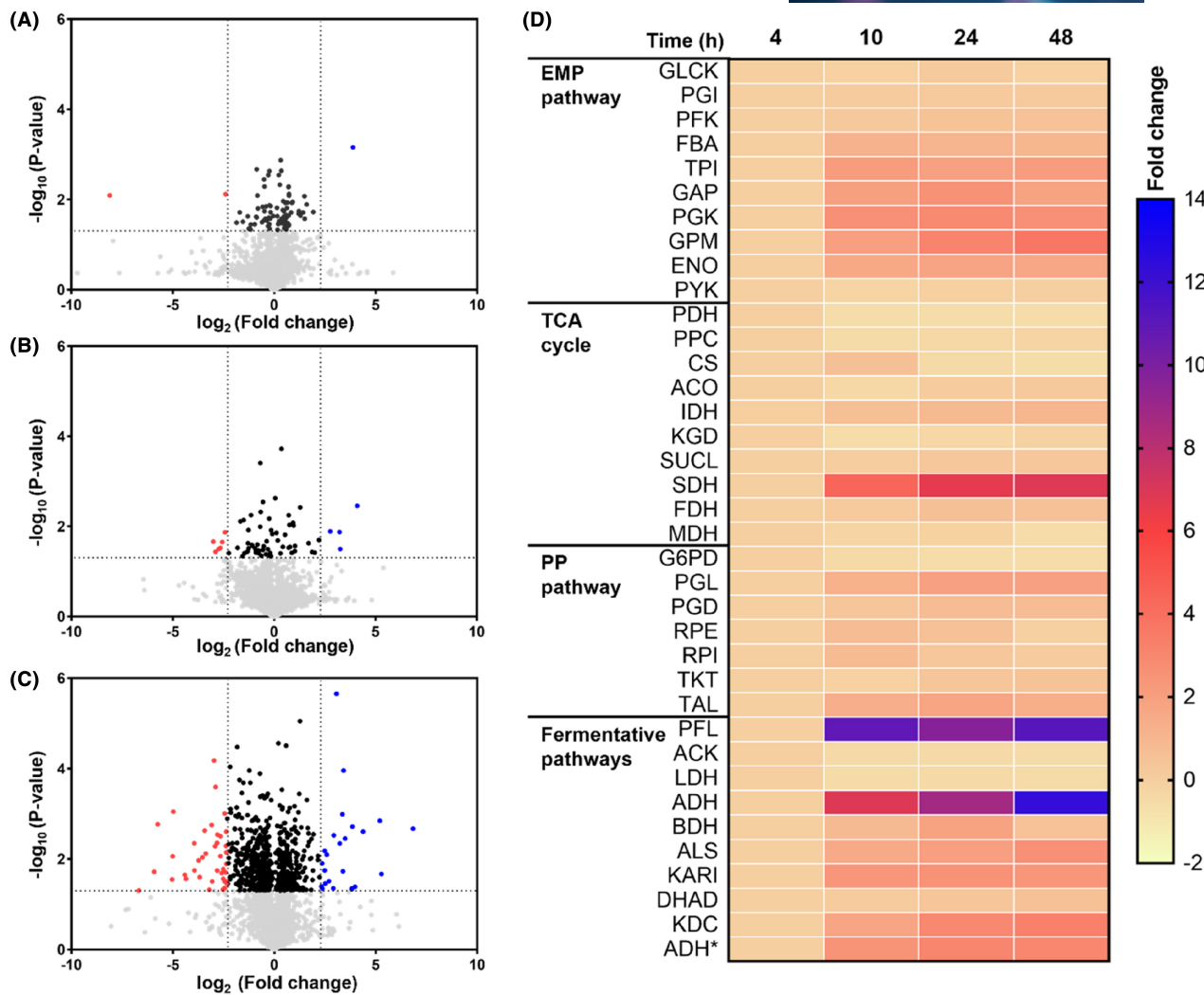


FIGURE 6 Network-wide proteomic analysis of *Paenibacillus polymyxa* strains. Investigation of the proteome of wild type (A) and Δ/dh (B) strains cultivated with and without isobutanol. (C) Proteome profiles of isobutanol-producing strain (Ppiso-5) in comparison to a non-producing strain (Δ/dh). Different colours represent the up- or downregulation of the corresponding proteins: black, up to 5-fold; red and blue, >5-fold. The X-axis represented the $-\log_{10}$ value of the calculated p-value and the Y-axis represented the \log_2 value of the fold change of one tested condition over the other. The horizontal dashed line indicates the cut-off $p < 0.05$. The area in between the vertical dashed lines represents the proteins change of up to 5-fold and the area outside these lines indicates >5-fold differential expression. (D) Proteome profiles of the central carbon metabolism and fermentative pathways of strain Ppiso-5 over the course of cultivation (4 h, early exponential; 10 h, late exponential; 24 and 48 h, stationary phase). The fold change was calculated relative to the level of the corresponding protein at 4 h.

metabolism was highly similar in the late exponential and stationary phases. Although we observed that the PP pathway was even upregulated by 17% between early and late stationary phases, which once again emphasized the importance of this pathway for NADPH regeneration.

Design of a minimal medium for *P. polymyxa* cultivation

So far *P. polymyxa* has been cultivated solely on rich media, which is economically costly and thus is unfavourable for large-scale applications. In this study, we systematically performed media optimization towards a

minimal synthetic medium for *P. polymyxa* cultivation. First, we evaluated the growth of the Ppiso-5 strain in rich medium (RM), or de Bont minimal medium (Hartmans et al., 1989) supplemented with either 0.05 g L^{-1} yeast extract (MM-YE) or 0.05 g L^{-1} peptone (MM-P). The strain was passaged directly from MM supplemented with 0.05 g L^{-1} YE and 0.1 g L^{-1} peptone into the indicated medium without prior adaption in order to also inspect possible adaption or lag phases. As expected, the best growth was obtained from the RM. However, despite a longer lag phase, the strain could also grow in MM-YE (biphasic), but not in MM-P. Since yeast extract contains a multitude of different compounds, such as amino acids and vitamins (Tomé, 2021), we decided to further investigate which of these compounds is

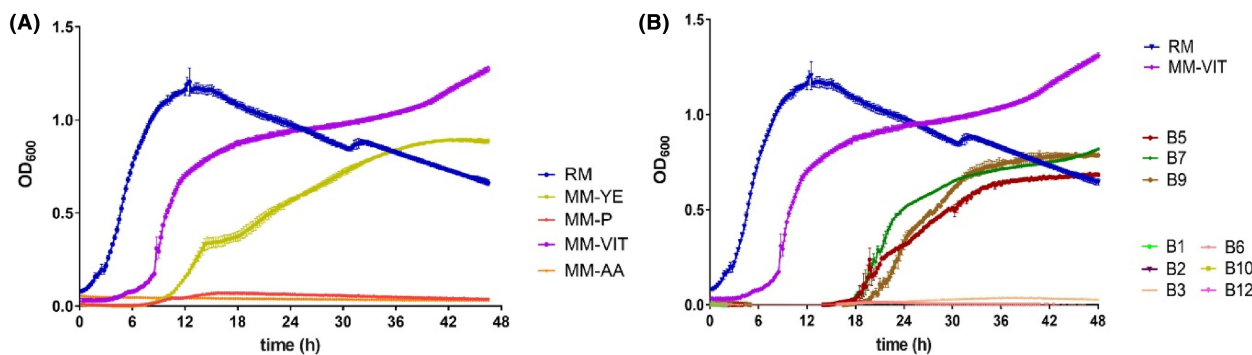


FIGURE 7 Culture medium optimization for *Paenibacillus polymyxa* cultivation. (A) Evaluating growth of strain Ppiso-5 in rich medium (RM) and de Bont minimal medium (MM) supplemented with diluted yeast extract (YE), peptone (P), vitamin B mix (VIT), or an amino acid mix (AA). (B) Investigating supplementation of single components of vitamin B and its impact on growth of strain Ppiso-5. The experiment was performed in 96-well microtiter plates. The graphs indicate mean values, and the error bars indicate standard deviation obtained from three biological replicates.

essential for *P. polymyxa* by supplementing more refined ingredients. No growth was observed from cultivation in minimal medium with the addition of a pure amino acid mix (MM-AA). Interestingly, the strain grew particularly well with the supplementation of vitamin B mix (MM-VIT) and maintained similar level of isobutanol production compared to the RM (Figure S7). Moreover, the strain showed a higher growth rate and shorter lag phase compared to MM-YE, and finally even reached a similar biomass concentration as in RM (Figure 7A; Table S12). This suggests that one or more components of the vitamin B mix promote growth of *P. polymyxa*. Subsequently, we cultivated the strain in MM supplemented with each component of vitamin B mix: B1, B2, B3, B5, B6, B7, B9, B10 or B12 (Figure 7B). It turned out that only pantothenate (B5), biotin (B7) and folate (B9) are essential for *P. polymyxa* to grow in MM. Genomic analysis of *P. polymyxa* revealed that many biotin biosynthetic genes are missing from its genome, which explains its auxotrophy for this vitamin. On the other hand, it was observed that supplementation of pantothenate or folate compensated growth even in the absence of biotin. It is plausible that these vitamins are linked through coenzyme A (CoA) and fatty acid biosynthesis, considering that pantothenate is the main precursor for CoA synthesis and biotin is the cofactor for several fatty acid biosynthetic enzymes (Leonardi & Jackowski, 2007; Sirithanakorn & Cronan, 2021). Furthermore, pantothenate generation requires 5,10-m ethylene-tetrahydrofolate, which is a derivative of folate (Chassagnole et al., 2003). Finally, the utilization of minimal medium would significantly reduce the cost of media for *P. polymyxa* cultivations (Table S13).

CONCLUSION

Paenibacillus polymyxa is a metabolically versatile organism which renders it a promising unconventional

prokaryotic host. In this study, we performed the first genome engineering for the implementation of a synthetic isobutanol pathway. Different mutants were generated by simultaneous integration of the isobutanol pathway and elimination of the native 2,3-BDO in *P. polymyxa*. A combinatorial approach of quantifying enzyme activity and proteomic analysis suggested that *ilvD*, which encodes for DHAD, was a main potential bottleneck of the synthetic pathway. Furthermore, engineering of the NADPH regeneration through overexpression of the malic enzyme improved the product titre to 1.5 g L⁻¹ isobutanol.

Proteomic analysis revealed a strong metabolic shift of *P. polymyxa* in response to isobutanol production. More than 600 proteins were found to be differentially expressed in the isobutanol-producing strain compared to the non-producing strain. Investigation of different growth phases of *P. polymyxa* identified a highly active TCA cycle in the early exponential phase, which subsequently shifted to upregulated glycolysis, PP pathway and fermentative pathways in the late exponential and stationary phases. However, an efficient NADPH regeneration via the PP pathway appeared to be limited by the low amount of G6PD enzymes.

Genomic analysis of *P. polymyxa* revealed that it lacks several biotin biosynthetic genes, which causes biotin auxotrophy. Through a series of media optimization rounds, we found out that supplementation of biotin restored the growth of *P. polymyxa* in minimal medium. Interestingly, the addition of pantothenate or folate resulted in a similar effect as biotin. We hypothesized that the three vitamins are interconnected through the CoA and fatty acid biosynthesis routes, and therefore, one component could compensate for the lack of the others. Finally, supplementation of vitamin B mix in the minimal medium improved the growth and shortened the lag phase compared to the addition of biotin, pantothenate and folate individually. The use of a minimal medium significantly reduced the media cost and thus

would increase the feasibility of *P. polymyxa* utilizations for larger scale applications.

AUTHOR CONTRIBUTIONS

Meliawati Meliawati: Conceptualization; formal analysis; investigation; methodology; writing – original draft; writing – review and editing. **Daniel C. Volke:** Methodology; project administration; supervision; writing – original draft; writing – review and editing. **Pablo I. Nikel:** Project administration; supervision; writing – original draft; writing – review and editing. **Jochen Schmid:** Conceptualization; funding acquisition; project administration; supervision; writing – original draft; writing – review and editing.

ACKNOWLEDGEMENTS

The authors thank Lizzie Eriksen and Marie V. Lukassen for their help in the preparation and measurement of the proteomics samples. The proteomic analysis was done at the DTU Proteomics Core. The authors also thank Moritz Gansbiller and Viviënne Mol for developing the analytical methods for isobutanol measurement, and Johannes Kabisch for the fruitful discussion. Open Access funding enabled and organized by Projekt DEAL.

FUNDING INFORMATION

MM acknowledges the funding from Erasmus+ Traineeship Grant (KA131) which supported her research stay at DTU Biosustain. This study is part of the German Federal Ministry of Education and Research (BMBF) funded project Polymore (project number 031B0855A). We acknowledge support from the Open Access Publication Fund of the Universität Münster.

CONFLICT OF INTEREST STATEMENT

The authors declare no conflicts of interest.

ORCID

Meliawati Meliawati  <https://orcid.org/0000-0003-2440-7000>

Pablo I. Nikel  <https://orcid.org/0000-0002-9313-7481>

Jochen Schmid  <https://orcid.org/0003-2557-5532>

REFERENCES

- Ankenbauer, A., Nitschel, R., Teleki, A., Müller, T., Favilli, L., Blombach, B. et al. (2021) Micro-aerobic production of isobutanol with engineered *Pseudomonas putida*. *Engineering in Life Sciences*, 21, 475–488.
- Atsumi, S., Hanai, T. & Liao, J.C. (2008) Non-fermentative pathways for synthesis of branched-chain higher alcohols as biofuels. *Nature*, 451, 86–89.
- Atsumi, S., Li, Z. & Liao, J.C. (2009) Acetolactate synthase from *Bacillus subtilis* serves as a 2-ketoisovalerate decarboxylase for isobutanol biosynthesis in *Escherichia coli*. *Applied and Environmental Microbiology*, 75, 6306–6311.
- Atsumi, S., Wu, T.Y., Eckl, E.M., Hawkins, S.D., Buelter, T. & Liao, J.C. (2010) Engineering the isobutanol biosynthetic pathway in *Escherichia coli* by comparison of three aldehyde reductase/alcohol dehydrogenase genes. *Applied Microbiology and Biotechnology*, 85, 651–657.
- Baez, A., Cho, K.M. & Liao, J.C. (2011) High-flux isobutanol production using engineered *Escherichia coli*: a bioreactor study with in situ product removal. *Applied Microbiology and Biotechnology*, 90, 1681–1690.
- Balcázar, J.L., Subirats, J. & Borrego, C.M. (2015) The role of biofilms as environmental reservoirs of antibiotic resistance. *Frontiers in Microbiology*, 6, 1–9.
- Basler, G., Thompson, M., Tullman-Ercek, D. & Keasling, J. (2018) A *Pseudomonas putida* efflux pump acts on short-chain alcohols. *Biotechnology for Biofuels*, 11, 1–10.
- Bastian, S., Liu, X., Meyerowitz, J.T., Snow, C.D., Chen, M.M.Y. & Arnold, F.H. (2011) Engineered ketol-acid reductoisomerase and alcohol dehydrogenase enable anaerobic 2-methylpropan-1-ol production at theoretical yield in *Escherichia coli*. *Metabolic Engineering*, 13, 345–352.
- Bayaraa, T., Gaete, J., Sutiono, S., Kurz, J., Lonhienne, T., Harmer, J.R. et al. (2022) Dihydroxy-acid dehydratases from pathogenic bacteria: emerging drug targets to combat antibiotic resistance. *Chemistry - A European Journal*, 28, e202200927.
- Beyer, L., Doberenz, C., Falke, D., Hunger, D., Suppmann, B. & Sawers, R.G. (2013) Coordination of FocA and pyruvate formate-lyase synthesis in *Escherichia coli* demonstrates preferential translocation of formate over other mixed-acid fermentation products. *Journal of Bacteriology*, 195, 1428–1435.
- Blombach, B. & Eikmanns, B.J. (2011) Current knowledge on isobutanol production with *Escherichia coli*, *Bacillus subtilis* and *Corynebacterium glutamicum*. *Bioengineered Bugs*, 2, 346–350.
- Blombach, B., Grünberger, A., Centler, F., Wierckx, N. & Schmid, J. (2021) Exploiting unconventional prokaryotic hosts for industrial biotechnology. *Trends in Biotechnology*, 40, 385–397.
- Bradford, M. (1976) A rapid and sensitive method for the quantitation of microgram quantities of protein utilizing the principle of protein-dye binding. *Analytical Biochemistry*, 72, 248–254.
- Brinkmann-Chen, S., Flock, T., Cahn, J.K.B., Snow, C.D., Brustad, E.M., McIntosh, J.A. et al. (2013) General approach to reversing ketol-acid reductoisomerase cofactor dependence from NADPH to NADH. *Proceedings of the National Academy of Sciences of the United States of America*, 110, 10946–10951.
- Callister, S.J., Barry, R.C., Adkins, J.N., Johnson, E.T., Qian, W., Webb-Robertson, B.-J.M. et al. (2006) Normalization approaches for removing systematic biases associated with mass spectrometry and label-free proteomics. *Journal of Proteome Research*, 5, 277–286.
- Chassagnole, C., Diano, A., Létisse, F. & Lindley, N.D. (2003) Metabolic network analysis during fed-batch cultivation of *Corynebacterium glutamicum* for pantothenic acid production: first quantitative data and analysis of by-product formation. *Journal of Biotechnology*, 104, 261–272.
- Colin, R., Ni, B., Laganenka, L. & Sourjik, V. (2021) Multiple functions of flagellar motility and chemotaxis in bacterial physiology. *FEMS Microbiology Reviews*, 45, 1–19.
- De La Plaza, M., Fernández De Palencia, P., Peláez, C. & Requena, T. (2004) Biochemical and molecular characterization of α-ketoisovalerate decarboxylase, an enzyme involved in the formation of aldehydes from amino acids by *Lactococcus lactis*. *FEMS Microbiology Letters*, 238, 367–374.
- Dickinson, J.R., Harrison, S.J. & Hewlins, M.J.E. (1998) An investigation of the metabolism of valine to isobutyl alcohol in *Saccharomyces cerevisiae*. *The Journal of Biological Chemistry*, 273, 25751–25756.
- Dickinson, J.R., Lanterman, M.M., Danner, D.J., Pearson, B.M., Sanz, P., Harrison, S.J. et al. (1997) A ¹³C nuclear magnetic

- resonance investigation of the metabolism of leucine to isoamyl alcohol in *Saccharomyces cerevisiae*. *The Journal of Biological Chemistry*, 272, 26871–26878.
- Dorau, R., Chen, L., Liu, J., Jensen, P.R. & Solem, C. (2019) Efficient production of α -acetolactate by whole cell catalytic transformation of fermentation-derived pyruvate. *Microbial Cell Factories*, 18, 1–11.
- Fu, C., Li, Z., Jia, C., Zhang, W., Zhang, Y., Yi, C. et al. (2021) Recent advances on bio-based isobutanol separation. *Energy Conversion and Management*: X, 10, 100059.
- Gehrman, S. & Tenhumberg, N. (2020) Production and use of sustainable C2-C4 alcohols – an industrial perspective. *Chemie-Ingenieur-Technik*, 92, 1444–1458.
- Gocke, D., Nguyen, C.L., Pohl, M., Stillger, T., Walter, L. & Müller, M. (2007) Branched-chain keto acid decarboxylase from *Lactococcus lactis* (KdcA), a valuable thiamine diphosphate-dependent enzyme for asymmetric C - C bond formation. *Advanced Synthesis and Catalysis*, 349, 1425–1435.
- Gu, P., Liu, L., Ma, Q., Dong, Z., Wang, Q., Xu, J. et al. (2021) Metabolic engineering of *Escherichia coli* for the production of isobutanol: a review. *World Journal of Microbiology and Biotechnology*, 37, 1–9.
- Gupta, J.A., Thapa, S., Verma, M., Som, R. & Mukherjee, K.J. (2020) Genomics and transcriptomics analysis reveals the mechanism of isobutanol tolerance of a laboratory evolved *Lactococcus lactis* strain. *Scientific Reports*, 10, 1–18.
- Hartmans, S., Smits, J.P., Van der Werf, M.J., Volkerling, F. & De Bont, J.A.M. (1989) Metabolism of styrene oxide and 2-phenylethanol in the styrene-degrading *Xanthobacter* strain 124X. *Applied and Environmental Microbiology*, 55, 2850–2855.
- Häßler, T., Schieder, D., Pfaller, R., Faulstich, M. & Sieber, V. (2012) Enhanced fed-batch fermentation of 2,3-butanediol by *Paenibacillus polymyxa* DSM 365. *Bioresource Technology*, 124, 237–244.
- Huo, Y., Zhan, Y., Wang, Q., Li, S., Yang, S., Nomura, C.T. et al. (2018) Acetolactate synthase (AlsS) in *Bacillus licheniformis* WX-02: enzymatic properties and efficient functions for acetoin/butanediol and I-valine biosynthesis. *Bioprocess and Biosystems Engineering*, 41, 87–96.
- Lennen, R.M., Lim, H.G., Jensen, K., Mohammed, E.T., Phaneuf, P.V., Noh, M.H. et al. (2023) Laboratory evolution reveals general and specific tolerance mechanisms for commodity chemicals. *Metabolic Engineering*, 76, 179–192.
- Leonardi, R. & Jackowski, S. (2007) Biosynthesis of pantothenic acid and coenzyme a. *EcoSal Plus*, 2, 73–80.
- Li, S., Huang, D., Li, Y., Wen, J. & Jia, X. (2012) Rational improvement of the engineered isobutanol-producing *Bacillus subtilis* by elementary mode analysis. *Microbial Cell Factories*, 11, 1–12.
- Lim, H.N., Lee, Y. & Hussein, R. (2011) Fundamental relationship between operon organization and gene expression. *Proceedings of the National Academy of Sciences of the United States of America*, 108, 10626–10631.
- Lin, P.P., Rabe, K.S., Takasumi, J.L., Kadisch, M., Arnold, F.H. & Liao, J.C. (2014) Isobutanol production at elevated temperatures in thermophilic *Geobacillus thermoglucosidasius*. *Metabolic Engineering*, 24, 1–8.
- Liu, X., Bastian, S., Snow, C.D., Brustad, E.M., Saleski, T.E., Xu, J.-H. et al. (2013) Structure-guided engineering of *Lactococcus lactis* alcohol dehydrogenase LIAdhA for improved conversion of isobutyraldehyde to isobutanol. *Journal of Biotechnology*, 164, 188–195.
- Meliawati, M., Teckentrup, C. & Schmid, J. (2022) CRISPR-Cas9-mediated large cluster deletion and multiplex genome editing in *Paenibacillus polymyxa*. *ACS Synthetic Biology*, 11, 77–84.
- Okonkwo, C.C., Ujor, V., Cornish, K. & Ezeji, T.C. (2020) Inactivation of the Levansucrase gene in *Paenibacillus polymyxa* DSM 365 diminishes exopolysaccharide biosynthesis during 2,3-butanediol fermentation. *Applied and Environmental Microbiology*, 86, 1–18.
- Okonkwo, C.C., Ujor, V.C., Mishra, P.K. & Ezeji, T.C. (2017) Process development for enhanced 2,3-butanediol production by *Paenibacillus polymyxa* DSM 365. *Fermentation*, 3, 1–15.
- Park, S.H., Kim, S. & Hahn, J.S. (2014) Metabolic engineering of *Saccharomyces cerevisiae* for the production of isobutanol and 3-methyl-1-butanol. *Applied Microbiology and Biotechnology*, 98, 9139–9147.
- Perez-Riverol, Y., Bai, J., Bandla, C., García-Seisdedos, D., Hewapathirana, S., Kamatchinathan, S. et al. (2022) The PRIDE database resources in 2022: a hub for mass spectrometry-based proteomics evidences. *Nucleic Acids Research*, 50, D543–D552.
- Petrov, K. & Petrova, P. (2021) Current advances in microbial production of acetoin and 2,3-butanediol by *Bacillus* spp. *Fermentation*, 7, 1–24.
- Qiu, M., Shen, W., Yan, X., He, Q., Cai, D., Chen, S. et al. (2020) Metabolic engineering of *Zymomonas mobilis* for anaerobic isobutanol production. *Biotechnology for Biofuels*, 13, 1–14.
- Rappaport, J., Mann, M. & Ishihama, Y. (2007) Protocol for micro-purification, enrichment, pre-fractionation and storage of peptides for proteomics using StageTips. *Nature Protocols*, 2, 1896–1906.
- Renna, M.C., Najimudin, N., Winik, L.R. & Zahler, S.A. (1993) Regulation of the *Bacillus subtilis* alsS, alsD, and alsR genes involved in post-exponential-phase production of acetoin. *Journal of Bacteriology*, 175, 3863–3875.
- Rütering, M., Cress, B.F., Schilling, M., Rühmann, B., Koffas, M.A.G., Sieber, V. et al. (2017) Tailor-made exopolysaccharides—CRISPR-Cas9 mediated genome editing in *Paenibacillus polymyxa*. *Synthetic Biology*, 2, 1–12.
- Schilling, C., Ciccone, R., Sieber, V. & Schmid, J. (2020) Engineering of the 2,3-butanediol pathway of *Paenibacillus polymyxa* DSM 365. *Metabolic Engineering*, 61, 381–388.
- Schilling, C., Klau, L.J., Aachmann, F.L., Rühmann, B., Schmid, J. & Sieber, V. (2022) Structural elucidation of the fucose containing polysaccharide of *Paenibacillus polymyxa* DSM 365. *Carbohydrate Polymers*, 278, 118951.
- Shi, A., Zhu, X., Lu, J., Zhang, X. & Ma, Y. (2013) Activating transhydrogenase and NAD kinase in combination for improving isobutanol production. *Metabolic Engineering*, 16, 1–10.
- Siripong, W., Wolf, P., Kusumoputri, T.P., Downes, J.J., Kocharin, K., Tanapongpipat, S. et al. (2018) Metabolic engineering of *Pichia pastoris* for production of isobutanol and isobutyl acetate. *Biotechnology for Biofuels*, 11, 1–16.
- Sirithanakorn, C. & Cronan, J.E. (2021) Biotin, a universal and essential cofactor: synthesis, ligation and regulation. *FEMS Microbiology Reviews*, 45, 1–18.
- Smit, B.A., Van Hylckama Vlieg, J.E.T., Engels, W.J.M., Meijer, L., Wouters, J.T.M. & Smit, G. (2005) Identification, cloning, and characterization of a *Lactococcus lactis* branched-chain α -keto acid decarboxylase involved in flavor formation. *Applied and Environmental Microbiology*, 71, 303–311.
- Smith, K.M. & Liao, J.C. (2011) An evolutionary strategy for isobutanol production strain development in *Escherichia coli*. *Metabolic Engineering*, 13, 674–681.
- Spaans, S.K., Weusthuis, R.A., van der Oost, J. & Kengen, S.W.M. (2015) NADPH-generating systems in bacteria and archaea. *Frontiers in Microbiology*, 6, 1–27.
- Stincone, A., Prigione, A., Cramer, T., Wamelink, M.M.C., Campbell, K., Cheung, E. et al. (2015) The return of metabolism: biochemistry and physiology of the pentose phosphate pathway. *Biological Reviews*, 90, 927–963.
- Su, Y., Zhang, W., Zhang, A. & Shao, W. (2020) Biorefinery: the production of isobutanol from biomass feedstocks. *Applied Sciences*, 10, 1–18.

- Tai, Y.S., Xiong, M., Jambunathan, P., Wang, J., Wang, J., Stapleton, C. et al. (2016) Engineering nonphosphorylative metabolism to generate lignocellulose-derived products. *Nature Chemical Biology*, 12, 247–253.
- Tomé, D. (2021) Yeast extracts: nutritional and flavoring food ingredients. *ACS Food Science & Technology*, 1, 487–494.
- Wei, J., Timler, J.G., Knutson, C.M. & Barney, B.M. (2013) Branched-chain 2-keto acid decarboxylases derived from *Psychrobacter*. *FEMS Microbiology Letters*, 346, 105–112.
- Werther, T., Spinka, M., Tittmann, K., Schütz, A., Golbik, R., Mrestani-Klaus, C. et al. (2008) Amino acids allosterically regulate the thiamine diphosphate-dependent α -keto acid decarboxylase from *Mycobacterium tuberculosis*. *The Journal of Biological Chemistry*, 283, 5344–5354.
- Wilbanks, B. & Trinh, C.T. (2017) Comprehensive characterization of toxicity of fermentative metabolites on microbial growth Mike Himmel. *Biotechnology for Biofuels*, 10, 1–11.
- Wirth, N.T., Funk, J., Donati, S. & Nikel, P.I. (2023) QurvE: user-friendly software for the analysis of biological growth and fluorescence data. *Nature Protocols*, 18, 2401–2403.
- Wushensky, J.A., Youngster, T., Mendonca, C.M. & Aristilde, L. (2018) Flux connections between gluconate pathway, glycolysis, and pentose-phosphate pathway during carbohydrate metabolism in *Bacillus megaterium* QM B1551. *Frontiers in Microbiology*, 9, 1–13.
- Yamamoto, S., Suda, M., Niimi, S., Inui, M. & Yukawa, H. (2013) Strain optimization for efficient isobutanol production using *Corynebacterium glutamicum* under oxygen deprivation. *Biotechnology and Bioengineering*, 110, 2938–2948.
- Yan, F., Yu, Y., Gozzi, K., Chen, Y., Guo, J. & Chai, Y. (2017) Genome-wide investigation of biofilm formation in *Bacillus cereus*. *Applied and Environmental Microbiology*, 83, 1–18.
- Zhan, Y., Xu, Y., Lu, X., Zhou, F., Zheng, P., Wang, D. et al. (2021) Metabolic engineering of *Bacillus licheniformis* for sustainable production of isobutanol. *ACS Sustainable Chemistry & Engineering*, 9, 17254–17265.

SUPPORTING INFORMATION

Additional supporting information can be found online in the Supporting Information section at the end of this article.

How to cite this article: Meliawati, M., Volke, D.C., Nikel, P.I. & Schmid, J. (2024) Engineering the carbon and redox metabolism of *Paenibacillus polomyxa* for efficient isobutanol production. *Microbial Biotechnology*, 17, e14438. Available from: <https://doi.org/10.1111/1751-7915.14438>